The Initial Mass Function of Early-Type Galaxies

Treu, Tommaso; Auger, Matthew W.; Koopmans, Leon V. E.; Gavazzi, Raphael; Marshall, Philip J.; Bolton, Adam S.

IMPORTANT NOTE: You are advised to consult the publisher's version (publisher's PDF) if you wish to cite from it. Please check the document version below.

Document Version
Publisher's PDF, also known as Version of record

[Link to publication in University of Groningen/UMCG research database](#)

THE INITIAL MASS FUNCTION OF EARLY-TYPE GALAXIES[1]

Tommaso Treu[2,3], Matthew W. Auger[2], Léon V. E. Koopmans[4], Raphaël Gavazzi[2,5], Philip J. Marshall[2], Adam S. Bolton[6,7]

submitted to ApJ

ABSTRACT

We determine an absolute calibration of the initial mass function (IMF) of early-type galaxies, by studying a sample of 56 gravitational lenses identified by the SLACS Survey. Under the assumption of standard Navarro, Frenk & White dark matter halos, a combination of lensing, dynamical, and stellar population synthesis models is used to disentangle the stellar and dark matter contribution for each lens. We define an "IMF mismatch" parameter $\alpha \equiv M_{*,\rm Ein}^{\rm LD}/M_{*,\rm Ein}^{\rm SPS}$ as the ratio of stellar mass inferred by a joint lensing and dynamical models ($M_{*,\rm Ein}^{\rm LD}$) to the current stellar mass inferred from stellar populations synthesis models ($M_{*,\rm Ein}^{\rm SPS}$). We find that a Salpeter IMF provides stellar masses in agreement with those inferred by lensing and dynamical models ($\langle \log \alpha \rangle = 0.00 \pm 0.03 \pm 0.02$), while a Chabrier IMF underestimates them ($\langle \log \alpha \rangle = 0.25 \pm 0.03 \pm 0.02$). A tentative trend is found, in the sense that α appears to increase with galaxy velocity dispersion. Taken at face value, this result would imply a non universal IMF, perhaps dependent on metallicity, age, or abundance ratios of the stellar populations. Alternatively, the observed trend may imply non-universal dark matter halos with inner density slope increasing with velocity dispersion. While the degeneracy between the two interpretations cannot be broken without additional information, the data imply that massive early-type galaxies cannot have both a universal IMF and universal dark matter halos.

Subject headings: gravitational lensing — galaxies: elliptical and lenticular, cD — galaxies: evolution — galaxies: formation — galaxies: structure

1. INTRODUCTION

The initial mass function (IMF) is a fundamental characteristic of a simple stellar population. Measuring the IMF from resolved stellar populations in the local universe has been a major astrophysical problem for decades (e.g., Salpeter 1955; Chabrier 2003).

From the point of view of understanding distant unresolved stellar populations, the IMF holds the key to interpreting observables such as colors and their evolution in terms of star formation history and chemical enrichment history. Among the many astrophysical problems where the IMF plays a key role, in this paper we will focus on the determination of the stellar mass of galaxies from the comparison of stellar populations synthesis models (e.g., Bruzual & Charlot 2003; Maraston 2005) with broad band colors. Stellar masses derived in this manner are often used to construct stellar mass functions and to study the demographics of galaxies over cosmic time (e.g., Brinchmann & Ellis 2000; Fontana et al. 2006; Bundy et al. 2006).

Unfortunately, the form of the IMF is degenerate with the derived stellar masses, since the luminosity is typically dominated by stars in a relatively narrow mass range. To facilitate comparison between results of different groups, it is therefore common practice to *assume* a standard, universal, and non-evolving IMF. Popular choices are the so-called Salpeter (1955) and Chabrier (2003) IMFs. However, this strategy leaves behind a systematic error that is believed to be of the order of a factor of two in stellar mass. Furthermore, the error need not correspond to a global error on the mean, but it could depend on the conditions of star formation and therefore for example on galaxy type, environment, metallicity and star formation epoch. Recent work, for example, has called into question the universality of the IMF and suggested it may be evolving with cosmic time (e.g., van Dokkum 2008; Davé 2008).

The goal of this paper is to determine the absolute normalization of stellar masses for early-type galaxies, its scatter from object to object, and its dependence on secondary parameters such as stellar velocity dispersion or stellar mass, by combining three independent probes of mass. Previous works have attempted to do this by comparing stellar masses determined from stellar populations synthesis models with those inferred from gravitational lensing (e.g., Ferreras et al. 2008) or stellar kinematics (e.g., Padmanabhan et al. 2004; Cappellari et al. 2006). However, the combination of the two latter techniques is particularly powerful as it allows one to reduce many of the degeneracies and disentangle the stellar and dark

[2] Department of Physics, University of California, Santa Barbara, CA 93106, USA (tt@physics.ucsb.edu, mauger@physics.ucsb.edu, pjm@physics.ucsb.edu)

[3] Sloan Fellow; Packard Fellow

[4] Kapteyn Institute, P.O. Box 800, 9700AV Groningen, The Netherlands (koopmans@astro.rug.nl)

[5] Institut d'Astrophysique de Paris, UMR7095 CNRS - Université Paris 6, 98bis Bd Arago, 75014 Paris, France (gavazzi@iap.fr)

[6] Beatrice Watson Parrent Fellow, Institute for Astronomy, University of Hawai'i, 2680 Woodlawn Dr., Honolulu, HI 96822 (bolton@ifa.hawaii.edu)

[7] Department of Physics and Astronomy, University of Utah, 115 South 1400 East, Salt Lake City, UT 84112 USA (bolton@physics.utah.edu)

component (e.g., Treu & Koopmans 2004).

To meet our goal we exploit the large and homogeneous sample of strong gravitational lenses discovered by the Sloan Lenses ACS Survey (Bolton et al. 2006; Treu et al. 2006; Koopmans et al. 2006; Gavazzi et al. 2007; Bolton et al. 2008a; Gavazzi et al. 2008; Bolton et al. 2008b; Auger et al. 2009). These papers showed that the SLACS lenses are statistically indistinguishable within the current level of measurement errors from control samples in terms of size, luminosity, surface brightness, location on the fundamental plane, environment, stellar and halo mass. Thus our results can be generalized to the overall population of early-type galaxies.

Recently, Grillo et al. (2009) used ground based photometry to derive stellar masses for a subset of SLACS lenses. They compared the inferred stellar mass fractions with average lensing stellar mass fractions determined by Koopmans et al. (2006) and Gavazzi et al. (2007) for subsamples of the SLACS lenses, finding a general agreement. The analysis presented here takes several steps forward: i) space-based HST photometry (Auger et al. 2009) extending into the near infrared is used for stellar masses; ii) individual stellar fraction estimates from lensing and dynamical models are used for each galaxy; iii) a Bayesian framework is adopted to determine the IMF normalization and errors for each galaxies. This progress allows us to investigate for the first time the scatter of the IMF and its possible dependency on galaxy velocity dispersion and hence, e.g., redshift of formation of the stellar populations or metallicity.

We assume a concordance cosmology with matter and dark energy density $\Omega_m = 0.3$, $\Omega_\Lambda = 0.7$, and Hubble constant $H_0 = 100h \mathrm{kms}^{-1}\mathrm{Mpc}^{-1}$, with $h = 0.7$ when necessary. Base-10 logarithms are used.

2. SAMPLE AND DATA

The sample analyzed in this paper is composed of 56 of the 58 early-type lens galaxies identified by the SLACS Survey, for which a joint lensing and dynamical analysis has been performed (§ 2.1), following the methods described by Treu & Koopmans (2004) and Koopmans et al. (2006). Two of the lenses of the Koopmans et al. (2009) sample have been excluded because the available single-band HST photometry is not sufficient to determine reliable stellar masses (Auger et al. 2009). All lenses are classified as definite (grade "A") based on the identification of multiple images and are successfully modeled as a single mass component. A full description of the SLACS Survey and the selection process — together with Hubble Space Telescope images and measured photometric and spectroscopic parameters of all the lenses — is given in the SLACS papers (Bolton et al. 2006, 2008a; Auger et al. 2009).

2.1. Dark and luminous mass from lensing and stellar kinematics

The lensing models provides a very accurate and precise measurement of the mass contained within the Einstein Radius (M_{Ein}). As discussed at length by, e.g., Treu & Koopmans (2004) and Koopmans et al. (2006), the addition of stellar velocity dispersion information allows one to disentangle stellar and dark matter, given a choice of mass models describing the dark matter halo,

the stellar component and orbital anisotropy. In practice, the joint lensing and dynamical analysis can be decoupled because the uncertainty on the lensing measurement is negligible with respect to that associated to the stellar velocity dispersion (see Barnabè et al. 2009, for joint analysis and detailed discussion of the methodology). We thus proceed as follows. First, we determine the total mass within the Einstein radius by fitting the lensing geometry with a gravitational lens model. The inferred lensing mass is determined to a few percent precision, independent of the specific form chosen to describe the gravitational potential of the deflector (assumed to be a singular isothermal ellipsoid by SLACS; Bolton et al. 2008a; Auger et al. 2009). We then compute the likelihood of a family of two-component mass models (stellar and dark matter) with respect to the stellar velocity dispersion measured by SDSS and determine the range of acceptable solutions by computing the posterior probability distribution function. Confidence intervals on each individual parameter can be obtained by marginalizing over the other parameters.

For the purpose of this paper, we adopt the so called NFW (Navarro et al. 1996, 1997) model for the dark matter halo:

$$\rho_{\mathrm{DM}}(r/r_b) = \frac{\rho_{\mathrm{DM},0}}{(r/r_{\mathrm{b}})(1 + (r/r_{\mathrm{b}}))^2}. \qquad (1)$$

In accordance with the CDM picture (e.g. Bullock et al. 2001, Macció et al. 2007) we expect the break radius r_b to be much larger than the effective and Einstein radii. This makes the results insensitive to the precise choice of r_b. We fix $r_b = 30$ kpc in agreement with the expected value for the average virial mass of the SLACS sample ($\sim 10^{13}$ $M_\odot$; Gavazzi et al. 2007).

The luminous component is described as either a Jaffe (1983) or a Hernquist (1990) model, which are good simple analytic descriptions of the light profile of early-type galaxies, and bracket the inner slope of the de Vaucouleurs (1948) profile. The orbital anistropy of the stars is modeled as a constant β

$$\beta \equiv 1 - \frac{\sigma_\theta^2}{\sigma_r^2}, \qquad (2)$$

where σ_θ and σ_r are the tangential and radial component of the pressure tensor. For clarity, we will adopt results obtained with Hernquist-isotropic models as our default (i.e., with $\beta = 0$). As we will discuss further below, none of the results of this paper is changed if Jaffe or moderately anisotropic models ($\beta = \pm 0.25$)– consistent with independent constraints on anisotropy (e.g. Gerhard et al. 2001) – are considered instead.

Since the mass within the Einstein radius is fixed by the lensing geometry– for a given anisotropy and functional form of the stellar component– the model has just one free parameter: the fraction of stellar mass f_* inside the cylinder of radius equal to the circularized Einstein radius. Thus, for each lens, the lensing and dynamical analysis produces the full posterior distribution function of f_*, $p(f_*)$, assuming a uniform prior in the interval [0,1]. The product of M_{Ein} and f_* provides the lensing+dynamical measurement of the stellar mass inside the Einstein Radius $M_{*,\mathrm{Ein}}^{\mathrm{LD}}$ for each lens galaxy. We note

that p(f_*), and thus p($M^{LD}_{*,Ein}$) are typically fairly asymmetric, because of the physical requirement that the stellar mass fraction be less or equal to unity imposed by the prior. For illustration purposes we use the median as our best estimator of the quantity, but we use the full distribution throughout the analysis. The average median value of f_* is 80% with a dispersion of 17%, consistent with the fact that most of the mass inside the Einstein Radius, corresponding on average to half the effective radius for the SLACS lenses, is accounted for by the stellar component.

The main goal of this paper is to explore the constraints on the IMF that can be gathered by *assuming* a standard universal NFW profile for the dark matter halo. More general forms of the dark matter halo profile could also be considered with our formalism, including for example the so-called generalized NFW profile, where the inner slope is allowed to be a free parameter. The gNFW profiled includes steeper profiles as well as profiles with a constant inner core, which are believed to be appropriate for some spiral and low surface brightness galaxies (e.g., Salucci et al. 2007, and references therein) as well as some clusters of galaxies (e.g. Sand et al. 2008; Newman et al. 2009, and references therein). In general, allowing the inner slope to be a free parameter results in a degeneracy between stellar mass fraction and inner slope (e.g., Treu & Koopmans 2004), in the sense that steeper inner slopes require less stellar mass to obtain the same stellar velocity dispersion. The degeneracy is best reduced by spatially resolved velocity dispersion measurements (e.g., Treu & Koopmans 2004). However, even with a single stellar velocity dispersion measurement, interesting limits on the inner slope and stellar mass fraction can be obtained by marginalizing over the other parameter with an appropriate prior. A full analysis of the inner slope of dark matter halos is left for future work when more accurate and spacially resolved velocity dispersion measurements will be available to better constrain the inner slope (e.g., Barnabé et al, 2010, in preparation). However, the results presented in this paper do not change significantly if a gNFW halo with uniform prior on the inner slope is considered instead of a simple NFW.

2.2. *Stellar mass from stellar populations synthesis models*

The second fundamental ingredient of this work is the posterior distribution function for the stellar mass derived by Auger et al. (2009) by applying stellar populations synthesis models to multicolor HST photometry. In this paper, we consider as our reference stellar masses based on the Bruzual & Charlot (2003) models using an informative prior on metallicity taken from the spectroscopic study of Gallazzi et al. 2005 (hereafter the Gallazzi prior; see Auger et al. 2009 for details). To check for possible systematics, we also consider stellar masses based on an "ignorant" uniform prior on metallicity (see Auger et al. 2009 for details), and based on stellar populations synthesis models by Maraston (2005). Finally, we consider two baseline choices of the IMF: the Chabrier (2003) and Salpeter (1955) models.

Taking into account the fraction of light inside the cylinder, this method provides an independent measurement of the stellar mass inside the Einstein radius $M^{SPS}_{*,Ein}$.

It is important to emphasize that the current stellar mass is significantly lower than the stellar mass at zero-age, due to mass loss during stellar evolution. For a single stellar population with Chabrier IMF, $\sim$50% of the initial mass is in the form of gas at 10 billions years of age. The fraction is significantly smaller for a Salpeter IMF ($\sim$30%), or if different prescriptions for stellar mass loss are adopted, as discussed, e.g., by Maraston (2005). Although the current stellar mass is the standard quantity for this kind of analysis it is clear that our joint lensing and dynamics analysis is sensitive to all the mass. Therefore, if a fraction of baryons lost during stellar evolution were to retain the phase space distribution of their parent stars, they would also be counted by the lensing and dynamical analysis towards the component distributed as light. Most of the residual gas in elliptical galaxies is believed to be currently in the hot phase, (e.g., Ciotti et al. 1991). The exact phase space distribution of the gas lost during stellar evolution depends on the complex interplay of winds, inflows and outflows, cooling, AGN heating, interactions with the environment and accretion of additional "unprocessed" gas (e.g., Pellegrini & Ciotti 1998; Pipino et al. 2005). Determining the fate of the gas is beyond the scope of this paper. However, X-ray observations show that the residual gas is a small fraction of the stellar mass (e.g. Mathews & Brighenti 2003; Humphrey et al. 2006) and therefore most of the gas must be either expelled or recycled into secondary episodes of star formation. For simplicity, in this analysis, we will consider two extrema that should bracket the exact solution. In our default scenario, all gas that is not recycled is dispersed and is therefore counted by our two component model in the dark matter halo. In this case, $M^{LD}_{*,Ein}$ needs to be compared with the current $M^{SPS}_{*,Ein}$ (including of course stellar remnants such as black holes and neutron stars). In the other extreme, all gas lost retains the distribution function of the stars and is therefore counted by the lensing and dynamical two-component model in the stellar component. In this latter case, which is effectively an upper limit to the dynamical importance of residual gas, $M^{LD}_{*,Ein}$ needs to be compared with $M^{SPS}_{*,Ein}$ at zero-age.

3. RESULTS

A comparison of the two independent determinations of stellar mass ($M^{LD}_{*,Ein}$ and $M^{SPS}_{*,Ein}$) is shown in Fig 1, for four combinations of IMF and lensing and dynamical models. The two quantities are tightly correlated, with scatter consistent with observational errors. Notice that for a Salpeter IMF the points lie on average around the identity line, and that changing anisotropy of stellar orbits has very little effects on the inferred $M^{LD}_{*,Ein}$. For a Chabrier IMF, in contrast, the current stellar mass underestimates that inferred from stellar populations synthesis models. Finally, the zero-age $M^{SPS}_{*,Ein}$ is larger than $M^{LD}_{*,Ein}$ even for a Chabrier IMF. The trends are robust with respect to the choice of stellar population synthesis models or metallicity priors, as illustrated in Figure 2. We note that the data appear to suggest that the relation between $M^{LD}_{*,Ein}$ and $M^{SPS}_{*,Ein}$ is not linear: at low masses the data appear to lie above the line indicating the identity, while at high masses the data appear to lie below
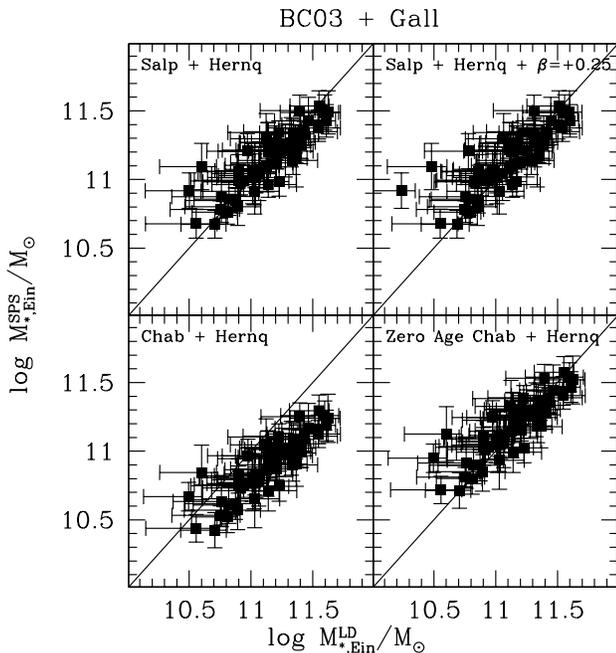
BC03 + Gall

FIG. 1.— Comparison between stellar mass in the cylinder of radius equal to the Einstein Radius as inferred from lensing and dynamical models (x-axis) and that inferred from fitting stellar populations synthesis models to the observed spectral energy distribution (y-axis). The solid line indicates the identity. Stellar populations synthesis models by Bruzual & Charlot (2003) are assumed together with an informative metallicity prior (Gallazzi et al. 2005).
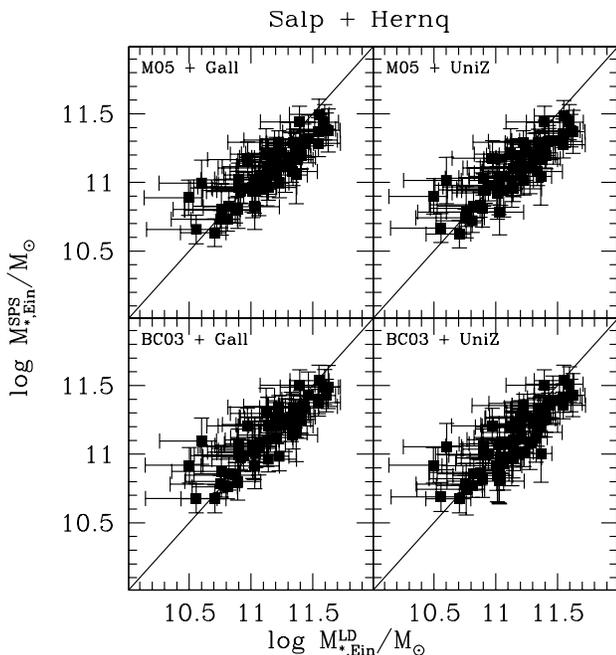
Salp + Hernq

FIG. 2.— As in Figure 1 for different choices of stellar population synthesis models and metallicity priors. Salpeter IMF and Hernquist stellar component models are assumed.

the identity. We will return to this point in Section 3.2 after we discuss in more detail the overall normalization in Section 3.1.
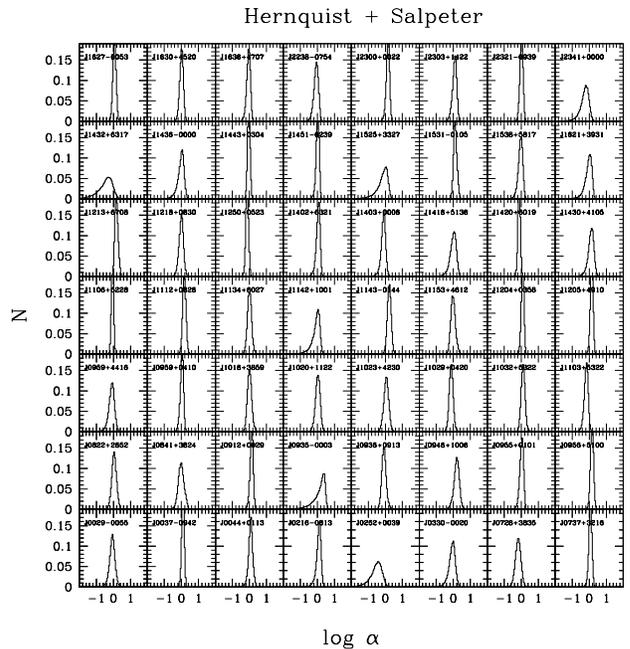
Hernquist + Salpeter

FIG. 3.— Posterior distribution function for the IMF mismatch parameter $\alpha \equiv M_{*,\mathrm{Ein}}^{\mathrm{LD}}/M_{*,\mathrm{Ein}}^{\mathrm{SPS}}$ with respect to a Salpeter IMF.

3.1. *Towards an absolute normalization of the IMF of massive galaxies: the "IMF mismatch" parameter*

The goal of this paper is to go beyond a comparison and determine the absolute normalization of the IMF for each galaxy. This is used to investigate its universality in terms of intrinsic scatter and dependency on galaxy parameters such as velocity dispersion (hence mass) and luminosity. For this purpose, we introduce an "IMF mismatch" parameter $\alpha \equiv M_{*,\mathrm{Ein}}^{\mathrm{LD}}/M_{*,\mathrm{Ein}}^{\mathrm{SPS}}$. For each galaxy, we determine the posterior distribution function for α by combining samples drawn from the posterior distribution function for $M_{*,\mathrm{Ein}}^{\mathrm{LD}}$ and from that for $M_{*,\mathrm{Ein}}^{\mathrm{SPS}}$. The resulting posterior distribution samples for α assuming Salpeter IMF are shown in Figure 3 for illustration. The median values of α for each lens are given in Table 1, together with other key properties of the lens galaxies, taken from Auger et al. (2009) and references therein.

The resulting average values of $\log \alpha$ for a variety of stellar population synthesis models are summarized in Table 2. The statistical uncertainty on $\langle \log \alpha \rangle$ is 0.03 dex for any given model. The different choices of dynamical model (Hernquist vs Jaffe, isotropic vs anisotropic) influence the average of $\log \alpha$ only at a level of 0.02, which can then be neglected in the rest of the discussion and considered as an additional systematic uncertainty. Confirming the trends shown in Figure 1, the statistical analysis shows that a Salpeter IMF tends to provide on average a much closer match between $M_{*,\mathrm{Ein}}^{\mathrm{SPS}}$ and $M_{*,\mathrm{Ein}}^{\mathrm{LD}}$ than a Chabrier IMF which appears to produce $M_{*,\mathrm{Ein}}^{\mathrm{SPS}}$ that are systematically lower than $M_{*,\mathrm{Ein}}^{\mathrm{LD}}$ (by $0.25 \pm 0.03 \pm 0.02$ dex).

Previous authors used comparisons between independent determinations of stellar masses to select one IMF versus another. For example, Grillo et al. (2009) concluded that the Chabrier IMF underestimates stellar

masses, and therefore preferred a Salpeter IMF, based on Bruzual & Charlot (2003) models. However, Grillo et al. (2009) only used the average dark matter fraction as published for a subset of the SLACS lenses and therefore could not make a detailed comparison for each individual case. We also note that the stellar masses inferred by Grillo et al. (2009) for the galaxies in common with this study are systematically different than the ones adopted here. As discussed by Auger et al. (2009), this difference is due to a combination of photometry differences, and choice of priors for metallicity and age parameters (e.g., Grillo et al. 2009 assume constant solar metallicity). However the differences are small and do not change the overall normalization, which is in very good agreement between the two studies.

In contrast, Cappellari et al. (2006) used different stellar populations synthesis models (Vazdekis et al. 1996) than the ones adopted here and found that stellar masses based on a Salpeter IMF were in some cases too high compared to those determined with stellar kinematics, reaching the opposite conclusion. However – in presence of significant statistical errors – this is actually expected, even if the Salpeter IMF were a perfect match to the intrinsic IMF, given that measurements will tend to scatter below and above the identity line. Indeed, even with our own method, there are systems for which $M_{*,\mathrm{Ein}}^{\mathrm{SPS}}$ exceeds $M_{*,\mathrm{Ein}}^{\mathrm{LD}}$ for a Salpeter IMF, even though the average of the median α is close to unity. Another caveat that must be kept in mind when comparing to the Cappellari et al. (2006) study is that their sample extends to significantly less massive galaxies than ours (velocity dispersions σ as low as 60 km s^{-1}, as opposed to our lower limit of approximately 200 km s^{-1}). Thus the two samples can only be compared directly if the IMF does not depend on velocity dispersion or on galaxy mass.

Regardless of the interpretation in terms of a specific IMF – which depends also on the uncertainties of the stellar populations models (e.g. Maraston 2005) – we emphasize that our method provides an absolute calibration of the stellar mass. The current stellar masses given in Auger et al. (2009) assuming a Salpeter IMF multiplied by α are *absolutely* calibrated against those inferred by the lensing and dynamical models. On average, the Auger et al. (2009) Salpeter masses are calibrated to within 0.04 dex, even without applying the IMF mismatch parameter. In general, the α values given in Table 1 can be used to calibrate any stellar population synthesis model, for any arbitrary choice of IMF, and destiny of the gas lost during stellar evolution. Remarkably, the data are consistent with *very little intrinsic scatter* in $\log \alpha$. The upper limit on the intrinsic scatter is 0.09 dex (95% CL), i.e. *the absolute normalization of the IMF is uniform to better than 25%.*

3.2. Universal or not? Trends with galaxy properties

Within the class of massive early-type galaxies, the SLACS lenses span approximately a factor of two in velocity dispersion and a factor of ten in luminosity and stellar mass (Auger et al. 2009). In turn, these quantities correlate with the average epoch of formation of their stellar populations, as well as their average metallicity, abundance ratios, and gas content (e.g., Treu et al. 2005; Thomas et al. 2005; Gallazzi et al. 2005; Jimenez et al.

2007; Pipino et al. 2009; Graves et al. 2009). If the IMF were to evolve during the epoch of formation of most of the stars of early-type galaxies, or if it were to depend on the mode of star formation or on the physical condition of the progenitor gas, we would expect α to vary across our sample.

To test for signs of mass dependency of the IMF normalization, we checked for a correlation between α and three indicators of galaxy "mass": i) σ_{SIE}, the velocity dispersion of the best fitting lensing model (Bolton et al. 2008a; Auger et al. 2009); ii) σ_*, the stellar velocity dispersion within the SDSS fiber aperture; iii) the total V band luminosity corrected to a common redshift $z = 0.2$ as described by Auger et al. (2009). The first two choices are motivated by several lines of evidence (e.g. Graves et al. 2009) that indicate that velocity dispersion is the most important parameter in determining stellar populations. The first quantity correlates well with stellar velocity dispersion and is measured much more accurately (Treu et al. 2006). The errors on σ_{SIE} are effectively negligible with respect to those on stellar velocity dispersion, which dominate the error on $M_{*,\mathrm{Ein}}^{\mathrm{LD}}$. Thus, this choice makes the covariance between α and σ_{SIE} negligible. The canonical stellar velocity dispersion σ_* suffers from a larger covariance with α due to its larger errors. The third quantity, the V-band luminosity, is an inferior galaxy mass proxy – because it is sensitive to relatively minor recent episodes of star formation – and is inversely covariant with α because to first order $M_{*,\mathrm{Ein}}^{\mathrm{SPS}}$ is proportional to L_V.

The results are shown in Figure 4 using the Salpeter IMF as baseline and for our standard stellar populations models (adopting a Chabrier IMF would move all the points upwards by ~ 0.25 dex, while all the other choices introduce negligible changes). A trend with non-zero slope is detected for σ_{SIE} and σ_*. No significant slope is found for L_V. The best fit linear relations are found to be, with no evidence of intrinsic scatter:

$$\log \alpha = (1.20 \pm 0.25) \log \sigma_{\mathrm{SIE}} - 2.91 \pm 0.02, \quad (3)$$

$$\log \alpha = (1.31 \pm 0.16) \log \sigma_* - 3.14 \pm 0.01, \quad (4)$$

$$\log \alpha = (0.11 \pm 0.08) \log L_V + 0.00 \pm 0.02, \quad (5)$$

where velocity dispersions are in units of km s^{-1} and L_V is in units of 10^{11} $L_{\odot,\mathrm{V}}$.

In summary, $\log \alpha$ appears to increase with velocity dispersion by an amount comparable to the difference between a Chabrier and Salpeter IMF over the range probed. The slope of the correlation with luminosity is significantly smaller then expected given the correlations with velocity dispersion and the Faber Jackson relation. The inverse covariance mentioned above is not sufficient to explain the discrepancy unless there is significant intrinsic scatter. This may therefore be another indication that velocity dispersion and not luminosity is the main parameter controlling stellar populations, including the IMF (Bernardi et al. 2007; Graves et al. 2009).
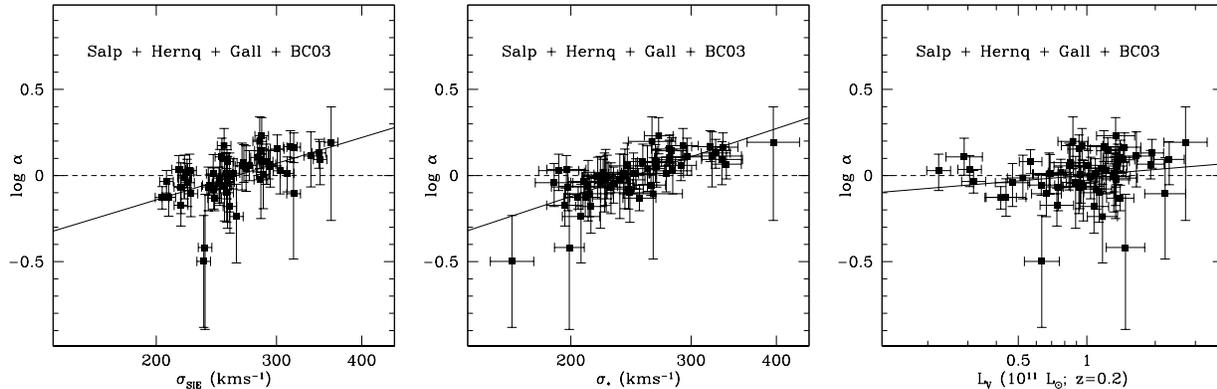
4. DISCUSSION

FIG. 4.— Template mismatch parameter $\alpha \equiv M^{\mathrm{LD}}_{*,\mathrm{Ein}}/M^{\mathrm{SPS}}_{*,\mathrm{Ein}}$ for Salpeter IMF as a function of lensing velocity dispersion (left), stellar velocity dispersion (center) and V-band luminosity corrected to $z = 0.2$. A tentative positive trend with velocity dispersion is observed (solid line). The dashed line represents the trend expected for a universal Salpeter IMF.

Before attempting to interpret our perhaps surprising findings, it is important to emphasize a number of caveats: i) the sample is relatively small and with a selection function that strongly favors high velocity dispersion galaxies; ii) the quantities on the two axis of Figure 4 are not independent, even though the known errors are small enough for covariance not to be causing the observed trends; iii) the stellar masses are typically based on three-band photometry and therefore we can only probe simple star formation histories. For all these reasons the results reported here must be considered as tentative until verified by larger samples, spanning a broader range of properties, and with the help of spectroscopic diagnostics of stellar populations.

Keeping these caveats in mind, we now discuss the two main results of this paper. The first result is that the average absolute normalization of the IMF inferred by our study is higher than those commonly assumed when deriving masses for distant galaxies using colors. Those "lighter" IMFs have been preferred on the basis of studies of local stellar populations (e.g. Kroupa 2001; Chabrier 2003) as well as on the basis of dynamical arguments applied to spiral galaxies (e.g. Bell & de Jong 2001). However, those measurements do not necessarily apply to the stellar populations of massive early-type galaxies, if the IMF is not universal, but depends, for example, on metallicity or other conditions that vary with cosmic time (e.g. Elmegreen 2008, and references therein). The second result is the trend in IMF normalization with galaxy velocity dispersion. Taken at face value, this trend would imply that whereas a "light" IMF such as Chabrier's is appropriate for systems with $\sigma \sim 200\,\mathrm{km\,s^{-1}}$ (and therefore more or less consistent with the standard conclusions for Milky-Way-type galaxies and spirals), for the most massive systems there is a higher abundance of low mass stars. This appears to be quite a dramatic change over a factor of ~ 2 in velocity dispersion, corresponding approximately to 0.15 dex change in [Fe/H] and 0.1 dex in [α/Fe] (Bernardi et al. 2006). Part of this trend could also be ascribed to larger fraction of gas loss during stellar evolution being retained by higher velocity dispersion systems. However, the amount of retained gas would have to be comparable to the stellar mass in the central regions in order to explain the trend completely,

which seems to be ruled out by X-ray observations (e.g. Mathews & Brighenti 2003). Deep X-ray observations of the SLACS sample would be useful to verify exactly how much gas is left. More and better spectroscopic data are needed to investigate whether this trend is real, or whether there are unknown systematic effects at play. If the trend were to be confirmed, it would have far reaching implications for the determination of the evolving mass function of galaxies, because it may change its shape as well as its overall normalization.

Alternatively – if the IMF normalization were indeed universal over the mass range spanned by the SLACS sample – our finding would imply that one of our assumptions in deriving $M^{\mathrm{LD}}_{*,\mathrm{Ein}}$ is not warranted. As we have shown, anisotropy or changes in the assumed stellar mass density profile are not going to be sufficient, as they only change α by a few hundredths of a dex at most. Only changing our assumed dark matter density profile systematically with σ would have a sufficiently large effect to affect the observed trend. The assumed break radius (and hence concentration parameter) has only minimal effects. The dominant parameter in determining f_* is the inner slope of the dark matter density profile γ: steeper halos require a smaller stellar mass fraction (see, e.g., Treu & Koopmans 2002; Koopmans & Treu 2003; Treu & Koopmans 2004). Thus – in order to keep α constant and consistent with a Chabrier normalization – dark matter halos would need to be NFW-like at the low end of the velocity dispersion range and become steeper towards the high end. In contrast – in order to keep α constant and consistent with a Salpeter normalization – dark matter halos would need to be NFW-like at the high end of the velocity dispersion range and become flatter towards the low end, tending towards an inner constant core.

What could cause the dark matter inner slope to steepen with velocity dispersion? Baryons are the primary suspect, since this trend is not observed in dark matter only simulations. Baryons are indeed dominant over this radial range, and they could be responsible for making the dark matter density profile steeper than NFW (e.g. Gnedin et al. 2004; Jiang & Kochanek 2007). This baryonic compression would need to be more effective for higher velocity dispersion objects in order to

explain the observed trend [8]. By steepening the dark matter density profile, baryons would also effectively increase the dark matter fraction within a fixed aperture. This in turn would imply a correlation between dark matter fraction and velocity dispersion.

5. CONCLUSIONS

We combined three independent diagnostics of mass (lensing, dynamics and stellar populations synthesis models) to determine an absolute normalization of the IMF for a sample of 56 early-type galaxies, spanning over a decade in stellar mass and a factor of two in velocity dispersion, under the assumption of a NFW dark matter density profile. On average, the absolute IMF normalization is found to be close to that of a Salpeter IMF and larger than that for a Chabrier IMF. Using the prescription outlined in this paper, stellar masses based on any stellar population synthesis models can be absolutely calibrated to better than 20%, a significant progress with respect to the range of a factor of ~ 2 spanned by standard choices of the IMF.

A tentative trend of IMF mismatch parameter $\alpha = M_{*,\mathrm{Ein}}^{\mathrm{LD}} / M_{*,\mathrm{Ein}}^{\mathrm{SPS}}$ with galaxy velocity dispersion is found. Two possible explanations, not necessarily mutually exclusive, are suggested for the observed trend:

- The IMF is not universal, but rather depends on parameters such as metallicity, age, and abundance ratios of the stellar populations. In order to fully explain the observed trend, the normalization of the IMF and thus the abundance of low mass stars, must increase from Chabrier-like for $\sigma \sim 200 \, \mathrm{km \, s^{-1}}$ to Salpeter-like for the most massive early-type galaxies.

- Dark matter halos are not universal. For a uniform Chabrier IMF, the observed trend of α with σ could be explained if the inner slope of the dark matter halo were systematically steeper than NFW for the high velocity dispersion systems. For a uniform Salpeter IMF, the the dark matter halos would have to be NFW at the high mass end and flatter at lower masses.

In conclusion, the data are inconsistent with both a universal IMF and universal NFW dark matter halos over the mass range probed by the SLACS sample. There is a fundamental degeneracy between the two interpretations that cannot be broken with the current dataset.

Further tests and more work are required to verify and extend our perhaps surprising results. Firstly, we need

to extend our samples to cover a wider range of redshifts, masses, and morphological types and thus probe a larger variety of IMFs. Secondly, we need to use spectral stellar population diagnostics to obtain independent constraints on the stellar mass to light ratios as well as on the physical parameters that may correlate with IMF normalization. Thirdly, we need to improve the constraints on the inner slope of the dark matter halo as a function of velocity dispersion to break the current degeneracy. At the level of individual galaxies, some progress can be achieved by constructing more sophisticated lensing and dynamical models (e.g., Barnabè et al. 2009). In fact, the models presented here only use a single measurement of stellar velocity dispersion from SDSS and the total mass enclosed by the Einstein Radius, while more radial information can be extracted from both diagnostics. At the level of joint analysis of sub samples of galaxies, we need to have enough objects so that they can be binned by velocity dispersions to perform a weak lensing analysis. The addition of weak lensing to the strong lensing, dynamics, and stellar populations diagnostics would allow us to probe systematic variations with velocity dispersion of the dark matter halo shape and of the stellar to virial mass to light ratio . If the amount of contraction is an important ingredient of the observed trend with velocity dispersion, we expect to see a parallel trend in the overall efficiency of converting baryons into stars, or perhaps in the spatial concentration of the stellar component relative to that of the halo.

---

[8] While this manuscript was under revision, we became aware of the work by Schulz et al. (2009) who find a similar trend based on a joint weak lensing and dynamical of early-type galaxies selected

from the SDSS survey.

REFERENCES

Auger, M. W., Treu, T., Bolton, A. S., Gavazzi, R., Koopmans, L. V. E., Marshall, P. J., Bundy, K., & Moustakas, L. A. 2009, ApJ, 705, 1099

Barnabè, M., Czoske, O., Koopmans, L. V. E., Treu, T., Bolton, A. S., & Gavazzi, R. 2009, MNRAS, 399, 21

Bell, E. F., & de Jong, R. S. 2001, ApJ, 550, 212

Bernardi, M., Hyde, J. B., Sheth, R. K., Miller, C. J., & Nichol, R. C. 2007, AJ, 133, 1741

Bernardi, M., Nichol, R. C., Sheth, R. K., Miller, C. J., & Brinkmann, J. 2006, AJ, 131, 1288

Bolton, A. S., Burles, S., Koopmans, L. V. E., Treu, T., Gavazzi, R., Moustakas, L. A., Wayth, R., & Schlegel, D. J. 2008a, ApJ, 682, 964

Bolton, A. S., Burles, S., Koopmans, L. V. E., Treu, T., & Moustakas, L. A. 2006, ApJ, 638, 703

Bolton, A. S., Treu, T., Koopmans, L. V. E., Gavazzi, R., Moustakas, L. A., Burles, S., Schlegel, D. J., & Wayth, R. 2008b, ApJ, 684, 248

Brinchmann, J., & Ellis, R. S. 2000, ApJ, 536, L77

Bruzual, G., & Charlot, S. 2003, MNRAS, 344, 1000

Bundy, K., Ellis, R. S., Conselice, C. J., Taylor, J. E., Cooper, M. C., Willmer, C. N. A., Weiner, B. J., Coil, A. L., Noeske, K. G., & Eisenhardt, P. R. M. 2006, ApJ, 651, 120

Cappellari, M., Bacon, R., Bureau, M., Damen, M. C., Davies, R. L., de Zeeuw, P. T., Emsellem, E., Falcón-Barroso, J., Krajnović, D., Kuntschner, H., McDermid, R. M., Peletier, R. F., Sarzi, M., van den Bosch, R. C. E., & van de Ven, G. 2006, MNRAS, 366, 1126

Chabrier, G. 2003, PASP, 115, 763

Ciotti, L., D'Ercole, A., Pellegrini, S., & Renzini, A. 1991, ApJ, 376, 380

Davé, R. 2008, MNRAS, 385, 147

de Vaucouleurs, G. 1948, Annales d'Astrophysique, 11, 247

Elmegreen, B. G. 2008, 388, 249

Ferreras, I., Saha, P., & Burles, S. 2008, MNRAS, 383, 857

Fontana, A., Salimbeni, S., Grazian, A., Giallongo, E., Pentericci, L., Nonino, M., Fontanot, F., Menci, N., Monaco, P., Cristiani, S., Vanzella, E., de Santis, C., & Gallozzi, S. 2006, A&A, 459, 745

Gallazzi, A., Charlot, S., Brinchmann, J., White, S. D. M., & Tremonti, C. A. 2005, MNRAS, 362, 41

Gavazzi, R., Treu, T., Koopmans, L. V. E., Bolton, A. S., Moustakas, L. A., Burles, S., & Marshall, P. J. 2008, ApJ, 677, 1046

Gavazzi, R., Treu, T., Rhodes, J. D., Koopmans, L. V. E., Bolton, A. S., Burles, S., Massey, R. J., & Moustakas, L. A. 2007, ApJ, 667, 176

Gerhard, O., Kronawitter, A., Saglia, R. P., & Bender, R. 2001, AJ, 121, 1936

Gnedin, O. Y., Kravtsov, A. V., Klypin, A. A., & Nagai, D. 2004, ApJ, 616, 16

Graves, G. J., Faber, S. M., & Schiavon, R. P. 2009, ApJ, 693, 486

Grillo, C., Gobat, R., Lombardi, M., & Rosati, P. 2009, A&A, 501, 461

Hernquist, L. 1990, ApJ, 356, 359

Humphrey, P. J., Buote, D. A., Gastaldello, F., Zappacosta, L., Bullock, J. S., Brighenti, F., & Mathews, W. G. 2006, ApJ, 646, 899

Jaffe, W. 1983, MNRAS, 202, 995

Jimenez, R., Bernardi, M., Haiman, Z., Panter, B., & Heavens, A. F. 2007, ApJ, 669, 947

Jiang, G., & Kochanek, C. S. 2007, ApJ, 671, 1568

Koopmans, L. V. E., et al. 2009, ApJ, 703, L51

Koopmans, L. V. E., & Treu, T. 2003, ApJ, 583, 606

Koopmans, L. V. E., Treu, T., Bolton, A. S., Burles, S., & Moustakas, L. A. 2006, ApJ, 649, 599

Kroupa, P. 2001, MNRAS, 322, 231

Maraston, C. 2005, MNRAS, 362, 799

Mathews, W. G., & Brighenti, F. 2003, ARA&A, 41, 191

Navarro, J. F., Frenk, C. S., & White, S. D. M. 1996, ApJ, 462, 563

—. 1997, ApJ, 490, 493

Newman, A. B., Treu, T., Ellis, R. S., Sand, D. J., Richard, J., Marshall, P. J., Capak, P., & Miyazaki, S. 2009, ApJ, 706, 1078

Padmanabhan, N., Seljak, U., Strauss, M. A., Blanton, M. R., Kauffmann, G., Schlegel, D. J., Tremonti, C., Bahcall, N. A., Bernardi, M., Brinkmann, J., Fukugita, M., & Ivezić, Ž. 2004, New Astronomy, 9, 329

Pellegrini, S., & Ciotti, L. 1998, A&A, 333, 433

Pipino, A., Chiappini, C., Graves, G., & Matteucci, F. 2009, MNRAS, 396, 1151

Pipino, A., Kawata, D., Gibson, B. K., & Matteucci, F. 2005, A&A, 434, 553

Sand, D. J., Treu, T., Ellis, R. S., Smith, G. P., & Kneib, J.-P. 2008, ApJ, 674, 711

Schulz, A. E., Mandelbaum, R., & Padmanabhan, N. 2009, submitted to MNRAS, arXiv:0911.2260

Salucci, P., Lapi, A., Tonini, C., Gentile, G., Yegorova, I., & Klein, U. 2007, MNRAS, 378, 41

Salpeter, E. E. 1955, ApJ, 121, 161

Thomas, D., Maraston, C., Bender, R., & Mendes de Oliveira, C. 2005, ApJ, 621, 673

Treu, T., Ellis, R. S., Liao, T. X., van Dokkum, P. G., Tozzi, P., Coil, A., Newman, J., Cooper, M. C., & Davis, M. 2005, ApJ, 633, 174

Treu, T., Koopmans, L. V., Bolton, A. S., Burles, S., & Moustakas, L. A. 2006, ApJ, 640, 662

Treu, T., & Koopmans, L. V. E. 2002, ApJ, 575, 87

—. 2004, ApJ, 611, 739

van Dokkum, P. G. 2008, ApJ, 674, 29

Vazdekis, A., Casuso, E., Peletier, R. F., & Beckman, J. E. 1996, ApJS, 106, 307

TABLE 1
BASIC PARAMETERS OF THE LENS GALAXIES

ID	z_l	σ_* (km s^{-1})	$\sigma_{\rm SIE}$ (km s^{-1})	L_V (z=0.2) (10^{11} M$_\odot$)	$\log\alpha$
J0029-0055	0.2270	229±18	217.3±5.0	0.69±0.05	$-0.07^{+0.14}_{-0.15}$
J0037-0942	0.1955	279±14	285.2±6.6	1.09±0.06	$0.09^{+0.07}_{-0.07}$
J0044+0113	0.1196	266±13	268.7±6.2	0.62±0.06	$0.08^{+0.11}_{-0.11}$
J0216-0813	0.3317	333±23	347.6±8.0	1.81±0.12	$0.09^{+0.10}_{-0.15}$
J0252+0039	0.2803	164±12	234.7±5.4	0.49±0.04	$-0.50^{+0.26}_{-0.38}$
J0330-0020	0.3507	212±21	251.7±5.8	0.74±0.07	$-0.06^{+0.15}_{-0.20}$
J0728+3835	0.2058	214±11	256.4±5.9	0.82±0.05	$-0.18^{+0.14}_{-0.16}$
J0737+3216	0.3223	338±17	292.5±6.7	1.51±0.09	$0.07^{+0.08}_{-0.09}$
J0822+2652	0.2414	259±15	270.8±6.2	0.87±0.06	$0.04^{+0.13}_{-0.13}$
J0841+3824	0.1159	225±11	247.9±5.7	0.96±0.09	$-0.01^{+0.17}_{-0.16}$
J0912+0029	0.1642	326±16	346.2±8.0	1.47±0.07	$0.13^{+0.08}_{-0.09}$
J0935-0003	0.3475	396±35	360.8±8.3	2.06±0.20	$0.19^{+0.20}_{-0.44}$
J0936+0913	0.1897	243±12	242.8±5.6	0.83±0.06	$-0.08^{+0.12}_{-0.12}$
J0946+1006	0.2219	263±21	283.5±6.5	0.66±0.04	$0.20^{+0.14}_{-0.16}$
J0955+0101	0.1109	192±13	223.8±5.1	0.17±0.01	$0.03^{+0.10}_{-0.12}$
J0956+5100	0.2405	334±17	318.0±7.3	1.12±0.08	$0.16^{+0.08}_{-0.09}$
J0959+4416	0.2369	244±19	253.6±5.8	0.86±0.06	$-0.10^{+0.14}_{-0.17}$
J0959+0410	0.1260	197±13	215.8±5.0	0.23±0.01	$0.04^{+0.08}_{-0.10}$
J1016+3859	0.1679	247±13	253.2±5.8	0.51±0.04	$0.01^{+0.12}_{-0.12}$
J1020+1122	0.2822	282±18	303.7±7.0	0.94±0.07	$0.03^{+0.13}_{-0.13}$
J1023+4230	0.1912	242±15	267.1±6.1	0.63±0.04	$0.06^{+0.13}_{-0.14}$
J1029+0420	0.1045	210±11	208.6±4.8	0.33±0.03	$-0.13^{+0.11}_{-0.11}$
J1032+5322	0.1334	296±15	249.6±5.7	0.22±0.02	$0.11^{+0.11}_{-0.11}$
J1103+5322	0.1582	196±12	217.4±5.0	0.56±0.04	$-0.17^{+0.10}_{-0.12}$
J1106+5228	0.0955	262±13	239.2±5.5	0.47±0.03	$-0.06^{+0.06}_{-0.06}$
J1112+0826	0.2730	320±20	314.4±7.2	0.90±0.06	$0.17^{+0.09}_{-0.09}$
J1134+6027	0.1528	239±12	242.4±5.6	0.52±0.04	$0.01^{+0.11}_{-0.12}$
J1142+1001	0.2218	221±22	254.3±5.8	0.68±0.04	$-0.04^{+0.15}_{-0.27}$
J1143-0144	0.1060	269±13	285.5±6.6	0.94±0.08	$0.23^{+0.11}_{-0.10}$
J1153+4612	0.1797	226±15	220.0±5.1	0.39±0.03	$-0.01^{+0.13}_{-0.12}$
J1204+0358	0.1644	267±17	253.9±5.8	0.44±0.02	$0.08^{+0.07}_{-0.07}$
J1205+4910	0.2150	281±14	285.2±6.6	0.96±0.05	$0.14^{+0.07}_{-0.08}$
J1213+6708	0.1229	292±15	251.4±5.8	0.68±0.06	$0.17^{+0.10}_{-0.08}$
J1218+0830	0.1350	219±11	254.0±5.8	0.78±0.07	$-0.01^{+0.11}_{-0.13}$
J1250+0523	0.2318	252±14	243.5±5.6	1.08±0.06	$-0.13^{+0.08}_{-0.07}$
J1402+6321	0.2046	267±17	293.7±6.8	1.05±0.05	$0.05^{+0.09}_{-0.12}$
J1403+0006	0.1888	213±17	224.8±5.2	0.50±0.03	$-0.11^{+0.11}_{-0.13}$
J1416+5136	0.2987	240±25	287.0±6.6	0.73±0.05	$0.01^{+0.15}_{-0.20}$
J1420+6019	0.0629	205±10	204.0±4.7	0.31±0.02	$-0.13^{+0.06}_{-0.07}$
J1430+4105	0.2850	322±32	336.9±7.7	1.28±0.10	$0.11^{+0.14}_{-0.18}$
J1432+6317	0.1230	199±10	235.8±5.4	1.10±0.09	$-0.41^{+0.31}_{-0.48}$
J1436-0000	0.2852	224±17	256.1±5.9	1.00±0.07	$-0.01^{+0.14}_{-0.21}$
J1443+0304	0.1338	209±11	207.0±4.8	0.24±0.01	$-0.03^{+0.06}_{-0.07}$
J1451-0239	0.1254	223±14	221.9±5.1	0.57±0.03	$0.02^{+0.08}_{-0.09}$
J1525+3327	0.3583	264±26	317.9±7.3	1.72±0.16	$-0.11^{+0.21}_{-0.37}$
J1531-0105	0.1596	279±14	281.4±6.5	1.02±0.08	$0.11^{+0.10}_{-0.08}$
J1538+5817	0.1428	189±12	222.3±5.1	0.36±0.03	$-0.04^{+0.11}_{-0.14}$
J1621+3931	0.2449	236±20	284.6±6.5	1.03±0.06	$-0.02^{+0.15}_{-0.22}$
J1627-0053	0.2076	290±15	273.8±6.3	0.79±0.05	$0.06^{+0.09}_{-0.09}$
J1630+4520	0.2479	276±16	311.1±7.2	1.04±0.05	$0.01^{+0.10}_{-0.11}$
J1636+4707	0.2282	231±15	247.2±5.7	0.73±0.05	$-0.05^{+0.10}_{-0.11}$
J2238-0754	0.1371	198±11	238.4±5.5	0.56±0.03	$-0.07^{+0.12}_{-0.14}$
J2300+0022	0.2285	279±17	300.8±6.9	0.72±0.04	$0.15^{+0.08}_{-0.10}$
J2303+1422	0.1553	255±16	289.7±6.7	1.03±0.05	$0.08^{+0.10}_{-0.13}$
J2321-0939	0.0819	249±12	259.1±6.0	0.78±0.05	$0.01^{+0.08}_{-0.09}$
J2341+0000	0.1860	207±13	262.0±6.0	0.89±0.06	$-0.24^{+0.19}_{-0.26}$

NOTE. — The IMF mismatch parameter α is given with respect to a Salpeter IMF assuming BC03 models and Gallazzi metallicity prior. σ_* is the SDSS-measured stellar velocity dispersion within the spectroscopic aperture, as given in SLACS paper V (Bolton et al. 2008a).

TABLE 2
Average IMF mismatch parameter
$(\langle \log \alpha \rangle)$

IMF	SSP models	Z Prior	$\langle \log \alpha \rangle$
Salpeter	BC03	Gallazzi	0.00
Chabrier	BC03	Gallazzi	0.25
Salpeter	BC03	Uniform	0.03
Chabrier	BC03	Uniform	0.27
Salpeter	M05	Gallazzi	0.05
Salpeter	M05	Uniform	0.06

Note. — Statistical errors are 0.03 dex.